Heidi Moe-Føre
SINTEF Fisheries and Aquaculture,
Postboks 4762 Sluppen,
Trondheim 7465, Norway
e-mail: Heidi.Moe.Fore@sintef.no

Per Christian Endresen
SINTEF Fisheries and Aquaculture,
Postboks 4762 Sluppen,
Trondheim 7465, Norway
e-mail: Per.Christian.Endresen@sintef.no

Karl Gunnar Aarsæther
SINTEF Fisheries and Aquaculture,
Postboks 4762 Sluppen,
Trondheim 7465, Norway
e-mail: Karl.Gunnar.Aarsather@sintef.no

Jørgen Jensen
SINTEF Fisheries and Aquaculture,
Postboks 4762 Sluppen,
Trondheim 7465, Norway
e-mail: Jorgen.Jensen@sintef.no

Martin Føre
SINTEF Fisheries and Aquaculture,
Postboks 4762 Sluppen,
Trondheim 7465, Norway
e-mail: Martin.Fore@sintef.no

David Kristiansen
SINTEF Fisheries and Aquaculture,
Postboks 4762 Sluppen,
Trondheim 7465, Norway
e-mail: David.Kristiansen@sintef.no

Arne Fredheim
SINTEF Fisheries and Aquaculture,
Postboks 4762 Sluppen,
Trondheim 7465, Norway
e-mail: Arne.Fredheim@sintef.no

Pål Lader
SINTEF Fisheries and Aquaculture,
Postboks 4762 Sluppen,
Trondheim 7465, Norway
e-mail: Pal.Lader@sintef.no

Karl-Johan Reite
SINTEF Fisheries and Aquaculture,
Postboks 4762 Sluppen,
Trondheim 7465, Norway
e-mail: Karl.Johan.Reite@sintef.no

Structural Analysis of Aquaculture Nets: Comparison and Validation of Different Numerical Modeling Approaches

The performance of three different numerical methods were compared and evaluated against data from physical model tests of nets subjected to a static load due to water currents. A parameter study of a simplified net cage model subjected to a steady flow was performed by all methods, varying the net solidity and the flow velocity. The three numerical methods applied models based on springs, trusses, or triangular finite elements. Hydrodynamic load calculations were based on the drag term in Morison's equation and the cross-flow principle. Different approaches to account for wake effects were applied. In general, the presented numerical methods should be able to calculate loads and deformations within acceptable tolerance limits for low to intermediate current flow velocities and net solidities, while numerical analyses of high solidity nets subjected to high current velocities tend to overpredict the drag loads acting on the structure. To accurately estimate hydrodynamic loads and structural response of net structures with high projected solidity, new knowledge and methods are needed. [DOI: 10.1115/1.4030255]

Introduction

Net cages for aquaculture have traditionally been dimensioned based on empirical data [1]. During the last decade, the requirements for documentation of net cage strength and deformation have increased, resulting in a demand for suitable methods for structural analysis [2]. A fish farm consists of several flexible interconnected components [3], making the analysis of a complete fish farm and its subcomponents a challenging task. The aquaculture net cage consists of a system of load carrying ropes enclosed by a netting material [3,4]. In structural analysis of nets, it is difficult to fully simulate the strong fluid–structure interaction between moving seawater and the highly flexible net (hydroelasticity). Further, the flow regime through and around net cages and the corresponding fluid–structure interaction is not fully investigated and understood [5].

Several methods have been suggested for hydrodynamic and structural analysis of nets, involving different structural elements

Contributed by the Ocean, Offshore, and Arctic Engineering Division of ASME for publication in the Journal of Offshore Mechanics and Arctic Engineering. Manuscript received August 25, 2014; final manuscript received March 26, 2015; published online April 16, 2015. Assoc. Editor: Hideyuki Suzuki.

and load models [2,6]. Today's state of the art numerical analysis methods has not been validated for high environmental loads, extremely large deformations, and high solidity net cages [7]. These are often the design criteria during an ultimate limit state condition [1].

Net solidity is defined as the relationship between the projected netting area and the total area of a net panel [1], and is given as a number between 0 and 1 (1 representing a solid fabric). The solidity is thus dependent on the twine thickness, the mesh size, and the shape of the joints [4]. Increasing solidities will lead to an increased tendency for the water to flow around a net cage rather than through it [5]. This will influence the hydrodynamic loads acting on the net cage. The loads acting on a rigid fixed net panel are highly dependent on the solidity of the netting material, and the loads will increase with increased solidity [8].

During seabased fish production, different biofouling organisms will grow on the net [9] and may have an effect on the hydrodynamic loads acting on the fish farm [10]. In Norway, the mandatory technical standard NS9415 [1] requires that biofouling should be accounted for in load calculations by increasing the twine thickness by 50% (in addition to the contribution to gravitational loads). Common netting materials have solidities in the range of 0.20–0.30, and netting materials with even higher solidities exist, meaning that we must be able to calculate loads on net cages with solidities up to at least 0.45.

In this paper, the performance of three different numerical methods are compared and evaluated against data from physical model tests [7]. The different numerical methods' ability to simulate the occurring net cage deformation, hydrodynamic loads, and fluid–structure interactions when exposed to static loads from water currents will be discussed.

Physical Net Cage Models and Loads

The physical net cage models were constructed as circular cylinders of square mesh netting (without bottom), representing simplified global models of nets for aquaculture. These models are suitable for validation of numerical codes, as the geometry is relatively simple to handle numerically. In addition, the netting twines are not scaled similarly to the global net dimensions, avoiding small Reynolds numbers and thus changes in flow regime compared to full scale. The rope structure was ignored, as the netting will be the main contributor to the generation of hydrodynamic loads due to its relatively large area. Model tests of net cylinders with various solidities were performed in April 2009 in the North Sea Centre Flume Tank in Hirtshals, Denmark, and are thoroughly documented in Moe-Føre et al. [7]. The tank contained fresh water with a density of approximately 1000 kg/m^3.

The net models had a diameter of 1.75 m and a wet unloaded depth of 1.50 ± 0.05 m. The upper circumference was fixed to a massive steel ring. Four different commercial Raschel knitted netting materials with polyamide six multifilaments were applied, described by the half mesh (length of mesh side) [4] and the measured twine thickness and solidity [7] in Table 1. The models were named as N19, N30, N35, and N43, reflecting the solidity of the applied material (Table 1). N19 and N30 were typical netting materials used in commercial full scale net cages, while N35 and N43 represent high solidity netting. Due to the practical limitations of the knitting machines, the high solidity was achieved by a small mesh size, rather than increasing the twine thickness. The netting materials N19 and N30 had a "super-knot" structure, while the two high solidity materials did not have this strengthened knot structure [3].

Table 1 Wet netting material dimensions

Net	Half mesh (mm)	Twine thickness (mm)	Solidity
N19	25.5	2.42	0.194
N30	16.2	2.35	0.302
N35	8.3	1.41	0.347
N43	5.8	1.35	0.434

Sixteen cylindrical steel weights with a diameter of 4 cm, a length of 6 cm, and a submerged weight of 4.48 N were evenly distributed around the lower circumference of the net model (Fig. 1). Tests showed that they had a drag coefficient of 1.1, although these short cylinders with free ends in theory should have a drag coefficient of about 0.7 for the actual flow regime [11].

The models were subjected to a close to uniform flow with seven different water current velocities ranging from 0.13 m/s to 0.93 m/s. A load cell attached to the center of the steel ring measured the reaction forces in six degrees-of-freedom. The load contribution from the steel ring was measured separately, and it was assumed that it could be subtracted from the reaction forces together with the weights in order to find the hydrodynamic loads acting on the net cage alone.

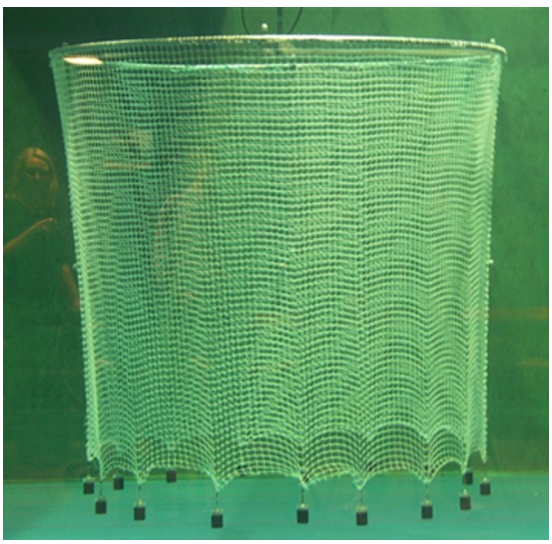

Fig. 1 Physical model test setup (N19, Table 1)

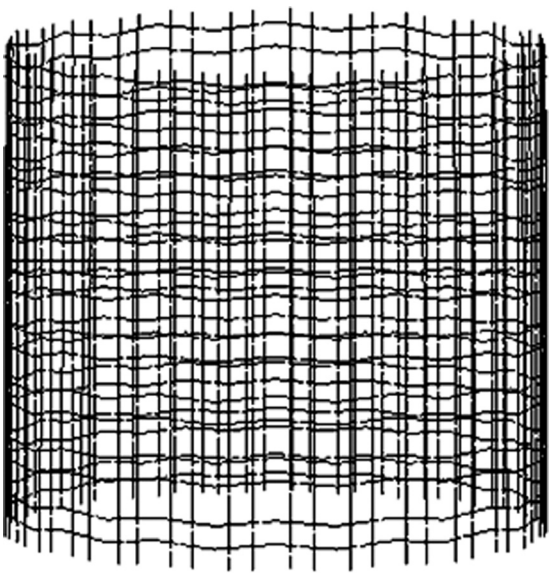

Fig. 2 Unloaded triangle model (elements are visualized with a grid simulating the netting structure)

Numerical Methods, Load and Cage Models

Three different finite element models were established based on the dimensions and properties of the physical models, and they were named after their element type (triangle, truss and spring, Figs. 2 and 3). The triangle and spring elements were implemented in the software framework FHSIM, developed at SINTEF Fisheries and Aquaculture [12], while the truss model was analyzed using ABAQUS Explicit and MATLAB.

All models were formulated as a set of differential equations, which were solved in the time-domain using numerical integration techniques. The equation of motion was established based on Newton's second law, requiring that nodal force resultants should equal nodal mass times acceleration. For all models, the hydrodynamic loads were calculated for each finite element and distributed over the nodes of the elements. Lumped mass formulation was applied, and point masses were defined at the nodes. An expression for the acceleration was derived from the equation of motion, and nodal displacements were found by integrating this. Different integration techniques were applied: Runge–Kutta 4–5 in the triangle method, the central difference rule for the truss model, while the spring model applied the Euler method. The static solution was found as the model reached steady-state, i.e., when total hydrodynamic loads acting on the system did not vary significantly for a constant flow velocity. At this point of convergence, the variation in load was below 2% for all methods. Stress and strain of an element were calculated based on the change in distance between interconnected mass points (nodes).

The numerical models were subjected to loads representing a uniform horizontal flow (in x-direction, Fig. 3) with the same undisturbed velocities as measured in the physical model tests. Load models were based on a Morison-type cross-flow drag [2,13], the loads were calculated using the drag term in Morison's equation and decomposed in local (element) and global axis systems.

The numerical models were restricted from any movement at the upper circumference. Linear elastic material properties with an E-modulus of 40 N/mm^2 were applied [14]. The netting density was 100 kg/m^3 higher than that of water.

Triangle Method and Model. The triangle method [13,15] modeled the net as triangular elements interconnected at the corners based on the element formulation by Priour [16]. Elements did not carry compressive loads in order to represent the behavior of netting materials with low bending stiffness, and geometry was updated at each time step.

The triangle model was created by defining 32 nodes equally distributed along the circumference and ten nodes over the depth of the model (see Fig. 2). A total of 576 triangular elements of equal size were defined between these nodes. These elements represented several twines (cylinders) and knots (spheres) in the netting. Twines were considered as circular cylinders during the hydrodynamic load calculations, and their diameter was found as the solidity times the half mesh divided by two. The twine thickness of N30 and N35 was by this increased by 3% compared to the measured values in Table 1, while the thickness of N43 was reduced by 7%. N19 was given a knot-diameter ratio of 1.5, meaning that the knot diameter was calculated as 1.5 times the diameter of the twine, while the other models applied a knot-diameter ratio of 1.0 (based on best fit to results from model tests).

Drag coefficient was given as a function of Rn for the twines [6], and flow velocity through the meshes was increased due to mass conservation (local speed-up, similar as in Ref. [6]). Tangential loads were calculated based on a tangential coefficient, $C_t = 0.01$. Drag loads from the weights were estimated using a standard drag formulation with $C_d = 1.1$ (based on experimental data [7]). Load calculations applied a fresh water density of 1000 kg/m^3.

Wake effects were included due to flow blockage caused by the netting [13]. Flow velocity was reduced after water had passed through a net panel (element) by a velocity reduction factor dependent on solidity and angle of attack. This was mainly experienced by the aft half of the net. In addition, local reduced velocity within a net panel due to blockage of upstream twines was included. This effect may be significant at low angles of attack (large net cage deformations). The method was based on Blevins virtual origin wake formulation for a circular cylinder [17] and combined according to Ref. [18] to obtain the total effect for a net panel [13].

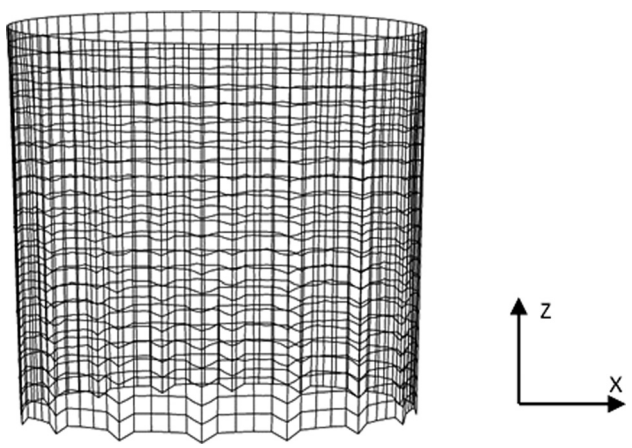

Fig. 3 Submerged truss model with bottom weights

Truss Method and Model. In the truss model [2,7], the net was modeled by three-dimensional truss elements (Fig. 3). All trusses were given a center node and would thus buckle under compression. Geometry was updated after several complete time simulations forming an iteration scheme. A series of simulations including the loads acting on the deformed model from the previous simulation were performed, until the differences in calculated drag and lift forces were less than 2% between the two last iterations.

The truss model consisted of 80 elements (160 nodes) of 68.73 mm around the circumference, and 23 elements (47 nodes) of 68.75 mm over the depth (Fig. 3). Each finite element represented several parallel twines in the netting and was given a cross-sectional area equal to the sum of the areas of the represented twines. Effects due to the joints (knots) were neglected. During the hydrodynamic load calculations, the netting was considered as a system of circular cylinders with a diameter equal to the thickness and a length equal to the half mesh given in Table 1.

Load calculations were based on a constant drag coefficient of $C_d = 1.15$ (derived from experimental data for netting of solidity 0.24 [2,18]) and fresh water density of 1000 kg/m^3. Tangential loads were neglected and drag loads from the weights were not applied. Wake effects due to the upstream part of the net were included at the downstream half of the numerical model by multiplying the flow velocity by a velocity reduction factor. The velocity reduction factor was found for the different net models as 64–87%, decreasing for increasing solidity. This was based on flow velocity measurements behind the physical model at an undisturbed water velocity of 0.39 m/s [7].

Spring Method and Model. The spring model was established based on the truss model input file, preserving the model topology and material properties. A nonlinear formulation of spring stiffness was implemented, allowing the springs to provide zero restoring force in compression, which eliminates the need of center nodes in this context. Geometry was updated at each time step, and the model dimensions and details were identical to the truss model (Table 1 and Fig. 3).

Load calculations were based on a constant drag coefficient of $C_d = 1.15$, a tangential coefficient $C_t = 0.01$, and seawater density

of 1025 kg/m^3. Drag loads from the weights were applied through a standard drag formulation with $C_d = 1.24$. Wake effects were included at the rear half of the undeformed numerical model through a velocity reduction factor similar as in the truss method.

Differences in Input Parameters. The three numerical methods included different input parameters with respect to water density, tangential load coefficients, and hydrodynamic loads from bottom weights. There was a 2% difference in depth between the triangle model (1.55 m) and the truss and spring models (1.58 m), and the twine thickness was different as described for the triangle model. These differences were considered to have a limited effect on the results, especially in the discussion of overall trends.

Results

Figures 4 and 5 show the detailed configuration of the triangle and truss model N30 for a uniform flow velocity of $v = 0.5$ m/s. The configuration of the spring model was similar to the truss model (Fig. 5). The shape of all physical models and corresponding truss models are shown and compared in the Appendix, and in general the numerical analyses seem to capture the behavior of a net cage.

Global deformations of the numerical net models are compared in Fig. 6, where the coordinates of the front and aft point of the top and bottom circumference have been plotted for calm water and three different flow velocities (0.26 m/s, 0.50 m/s, and 0.93 m/s). The initial shape in calm water is shown with the effect of bottom weights and gravity for the truss model, while the triangle and spring models are shown without the effect of loads in calm water.

For the low solidity N19, the numerical models yielded similar global deformations, and compared to the photographs from the physical model tests (see Appendix) they seem to slightly overpredict the horizontal and vertical translations of the net. Due to possible differences in the perspectives of the image, no firm conclusions have been made. The global deformation of the truss and spring model is in general similar, and the small difference is mainly due to the fact that the truss model does not apply drag loads from the bottom weights in the simulations. For higher solidities, the deformation of the truss model seem to be more in accordance with the physical model, while the triangle model overpredicts the net deformations, except at high velocities (0.93 m/s) where the deformation is similar for all numerical models. The deformation does not increase in direct proportion to the flow velocity, however, results indicate that the net deformation tends toward a constant limit state configuration, independent on flow velocity, as the velocity increases [7]. There are no results for the truss model N43 for velocities above 0.65 m/s due to convergence issues.

The contribution to drag and lift forces from the net model alone is presented in Fig. 7. (Contributions from steel ring system and weights were subtracted from the measurements.) Drag and lift forces are given as the horizontal and vertical components of the reaction forces at the upper circumference (steel ring) due to

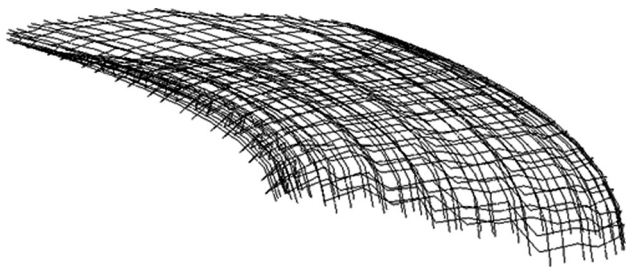

Fig. 4 Triangle model N30 subjected to a uniform flow, $v = 0.50$ m/s

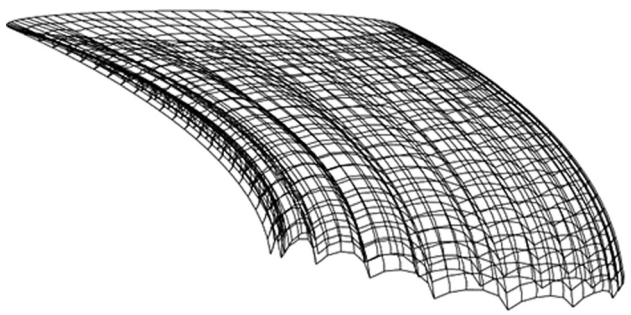

Fig. 5 Truss model N30 subjected to a uniform flow, $v = 0.50$ m/s

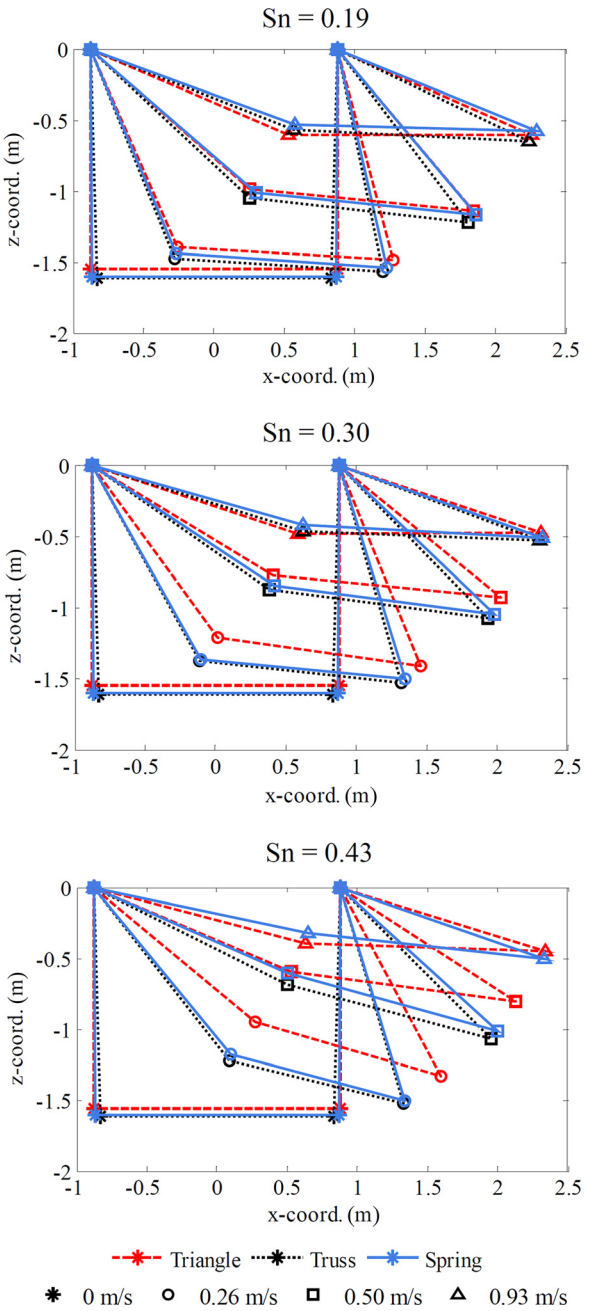

Fig. 6 Global deformation of the numerical models with various solidities subjected to various flow velocities

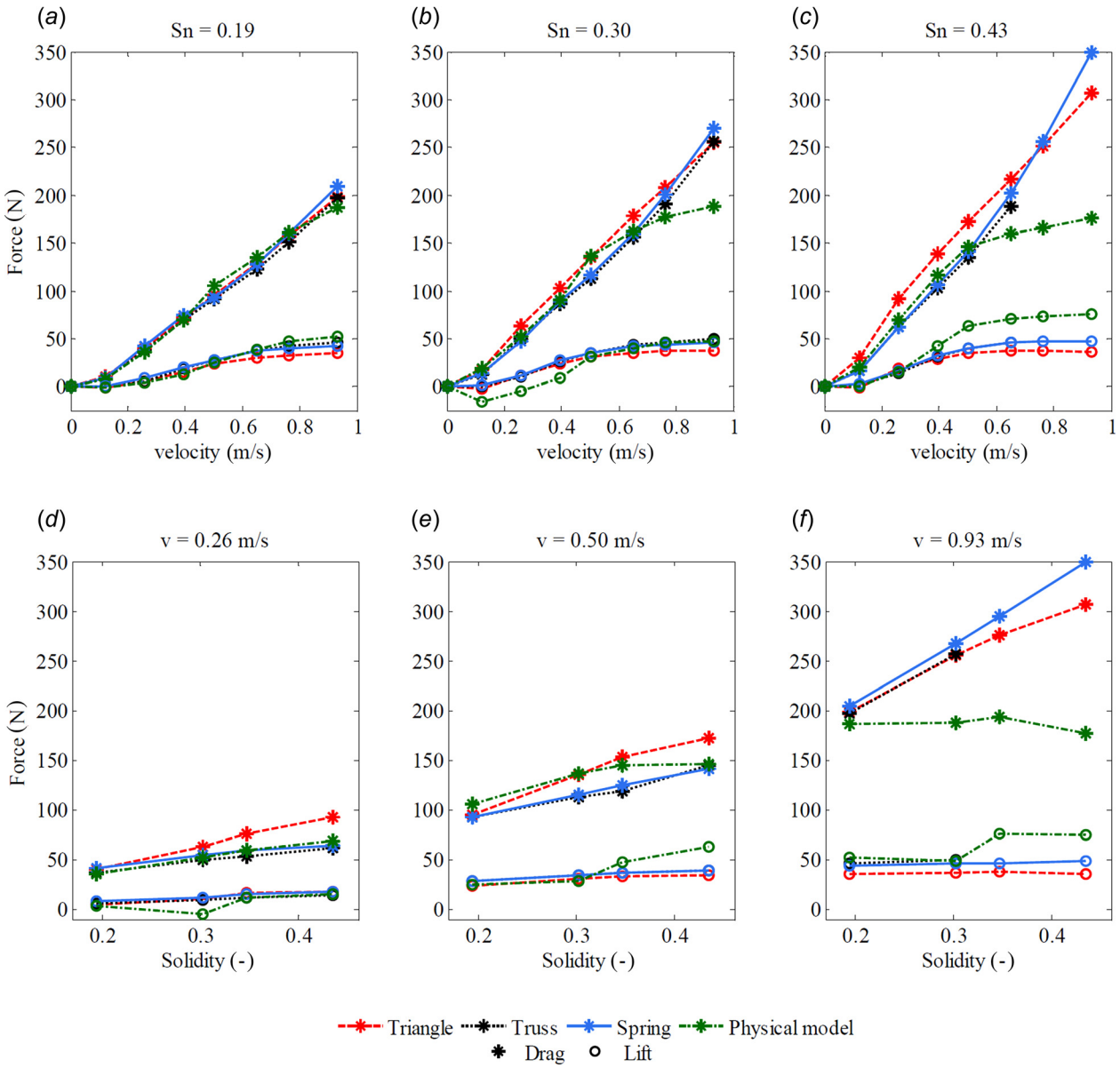

Fig. 7 Calculated and measured drag and lift forces. The numerical results are named by their element type (triangle, truss, and spring). (*a*)–(*c*) Forces are given as a function of flow velocity for different solidities (Sn). (*d*)–(*f*) Forces are given as a function of solidity for different flow velocities (*v*).

the hydrodynamic loads acting on the net cage. All numerical methods yielded similar hydrodynamic forces for the low solidity N19, and these were close to the results from the physical model tests. However, it is important to notice that the truss and spring models did not yield conservative estimates for all velocities. This may be adjusted through increasing the drag coefficient, which may be too low for low Reynolds numbers (low velocities). For high solidity cages, all numerical analysis overpredicted drag loads for high velocities, while lift loads were underpredicted compared to the physical model test results. Estimated drag was up to twice as high as the measured drag for the highest solidity net. The drag versus velocity curves from the physical model tests bend at approximately 0.5 m/s, and they continue with a less steep slope for increasing velocities. At the same velocity, the measured lift loads are close to the weight of the netting and bottom weights for N35 and N43 (approximately 75 N, Ref. [7]), meaning that the resulting vertical load component acting on the net and weight system is close to zero. Although the triangle method shows a slight change in slope, this is a trend which the numerical models were not able to recreate.

Analyses of the spring and truss models gave similar drag and lift loads, and the small differences were probably mainly due to the difference in applied water density and drag loads from the bottom weights.

The hydrodynamic loads showed a lower dependency on solidity in the physical model tests than in the numerical analyses. For N30, negative lift loads were measured. This may in theory be due to measurement errors, high viscous loads (friction) and deflection of flow. It is questioned whether these results are valid [7].

Discussion

The presented numerical methods should be able to calculate loads and deformations within acceptable tolerance limits for low to intermediate current flow velocities and net solidities, while numerical analyses of high solidity nets subjected to high current velocities tend to overpredict the drag loads acting on the structure. The quality of the numerical analysis depends on the choice of drag coefficient, i.e., how well the hydrodynamic drag loads are estimated for different Reynolds numbers.

Uncertainties and errors will always affect the quality of the results from physical model tests, as well as numerical analyses. The physical model tests applied in the current work involved uncertainties and errors due to imperfect model geometries, nonuniform water flow and measurement errors [2,7]. Together, these uncertainties and errors may represent deviations in measured loads and translations of several percentages compared to a perfect system. In order to achieve a sufficient validation of the applied numerical methods for low to intermediate hydrodynamic loads, comparisons with other model tests, preferably from other laboratories and models, should be applied. Introducing physical experiments with different uncertainties and errors into the assessment of the quality of the numerical estimates will thus be of importance.

The probable cause of the measured limited increase in drag with increasing flow velocity for high velocities is that the water will flow under and around the net to a larger extent, rather than through it. As solidity increases, the presence of the net may lead to global changes in the flow, both due to increased twine thickness versus mesh size ratio and net deformations. The results concur with findings in Ref. [5], where flow through and around stiff cylinders with various solidity was studied. This aspect of the fluid–structure interaction, where the structure significantly affects the global fluid behavior, is not included in the numerical analysis. It can thus be seen that the calculated drag loads continue to increase at a high rate with increasing flow velocities. The numerical methods, and especially the wake model applied for the triangular elements, will take the deformation of the net into account when calculating the loads, but they are not able to fully handle the changed flow.

Results for the triangle model differ from the results of the truss and spring model, which are similar. The triangle model yielded higher drag for low velocities, lower drag for high velocities and in general lower lift loads. This probably also led to a too large estimated deformation of the net model. These deviations may be due to differences in numerical load models and modeled wake effects. The triangle model seeks to include changes in flow in more detail by modeling local speed-up between twines, local wake effects and a reduction factor for the aft part of the net that is dependent on deformation of the net. The local speed-up will lead to higher hydrodynamic loads and thus larger deformations. For an increased projected solidity, i.e., large deformations and low angles of attack in parts of the net, the local speed-up may in addition yield a too high water velocity through the meshes as the water in reality might be deflected [19]. This effect will be valid for all models, but the effect will be stronger when local speed-up is accounted for.

In general, the estimated drag loads increased for increasing flow velocity. However, at high velocities, the drag from the triangle method increased at a lower rate than for the other numerical models. This was probably due to implementation of a geometry dependent reduced velocity factor that increased for increasing inclination of the front part of the net. Local wake effects, which occurs at large deformations, may also have contributed. The wake effect in the triangle model will vary with deformation of the net, and will be different in different sections. A direct comparison between the constant reduced velocity approach of the truss and spring models would be a comprehensive task. However, considering a net panel with a 45 deg inclination, the applied reduced velocity factor is larger for the triangle model than the other two models.

Based on the discussion above, it is possible that the overestimation of drag loads for the triangle model at low to intermediate velocities and the too large deformation is due to the modeled local speed-up between the twines. It may not be correct to include these local changes in flow without taking the global changes in flow into account, as they will interact. In addition, the effect of the modeled speed-up on the hydrodynamic loads may be too large.

The spring model in FHSIM seems to be the most efficient method with low computational time. The uniaxial truss and spring of elements are also suitable for modeling of the typical square mesh netting found in most net cages for Norwegian aquaculture. Net cage analysis using FhSim also benefit by a solid load model for hydrodynamic analysis, however, the methods studied in this work are in need of more validation and more refined fluid–structure interaction models for calculation of nets with high solidities and/or large deformations.

Conclusion

The presented numerical methods should be able to calculate loads and deformations within acceptable tolerance limits for low to intermediate current flow velocities and net solidities, while numerical analyses of high solidity nets subjected to high current velocities tend to overpredict the drag loads acting on the structure.

None of the numerical methods were fully able to reproduce the hydrodynamic loads and behavior found in the physical model tests. All methods showed strengths and weaknesses. The uniaxial truss and spring elements seemed computational effective. The wake model implemented with the triangular elements seem promising, especially by introducing local wake effects.

To accurately estimate hydrodynamic loads and structural response of net structures with high projected solidity, new knowledge and methods are needed. Further development and validation of numerical methods are required.

Acknowledgment

This work was funded by the Norwegian Research Council through the research platform Secure (securing fish-farming technology and operations to reduce escapes) and the NumSim project (numerical simulation of complex systems involving interaction between elements with large and varying stiffness properties). FhSim and implemented models are mainly developed through research projects funded by the Norwegian Research Council.

Nomenclature

C_d = drag coefficient (normal to element)
C_t = tangential drag coefficient (viscous friction)
r = velocity reduction factor, velocity behind net panel divided by velocity in front of net panel
Rn = Reynolds number, the ratio between inertia forces and viscous forces in the fluid
Sn = solidity, the ratio between the projected netting material area and the total area of a netting panel
v = undisturbed water flow velocity

Appendix: Deformation of Net Cage Models

Deformation of the physical net model was documented by photographs, and in this Appendix, they are compared with corresponding deformed configuration of a modified truss element model (Fig. 8). For the purpose of comparing the deformed shape of the different models, a series of analyses of the truss model with applied drag loads from the bottom weights were performed (modified truss method). This series of tests involved N19, N30, and N43 subjected to a uniform current flow with a velocity of 0.5 m/s. Assessing the global deformation of the modified truss model (Fig. 6), there is an almost perfect match between the modified truss method and the spring method. The physical models are outlined and the same contours are applied to the corresponding numerical results in Fig. 8. The horizontal and vertical deformation increased with increasing solidity. The modified truss model captured the shape well, however the vertical translation seem to be overpredicted, which is also the case for the horizontal translation for N19. However, no firm conclusions can be made as it is not possible to objectively assess the perspectives of the photographs and plots and thus whether they match. The photograph of the high solidity N43 shows an asymmetrical deformation, which is discussed in Ref. [7].

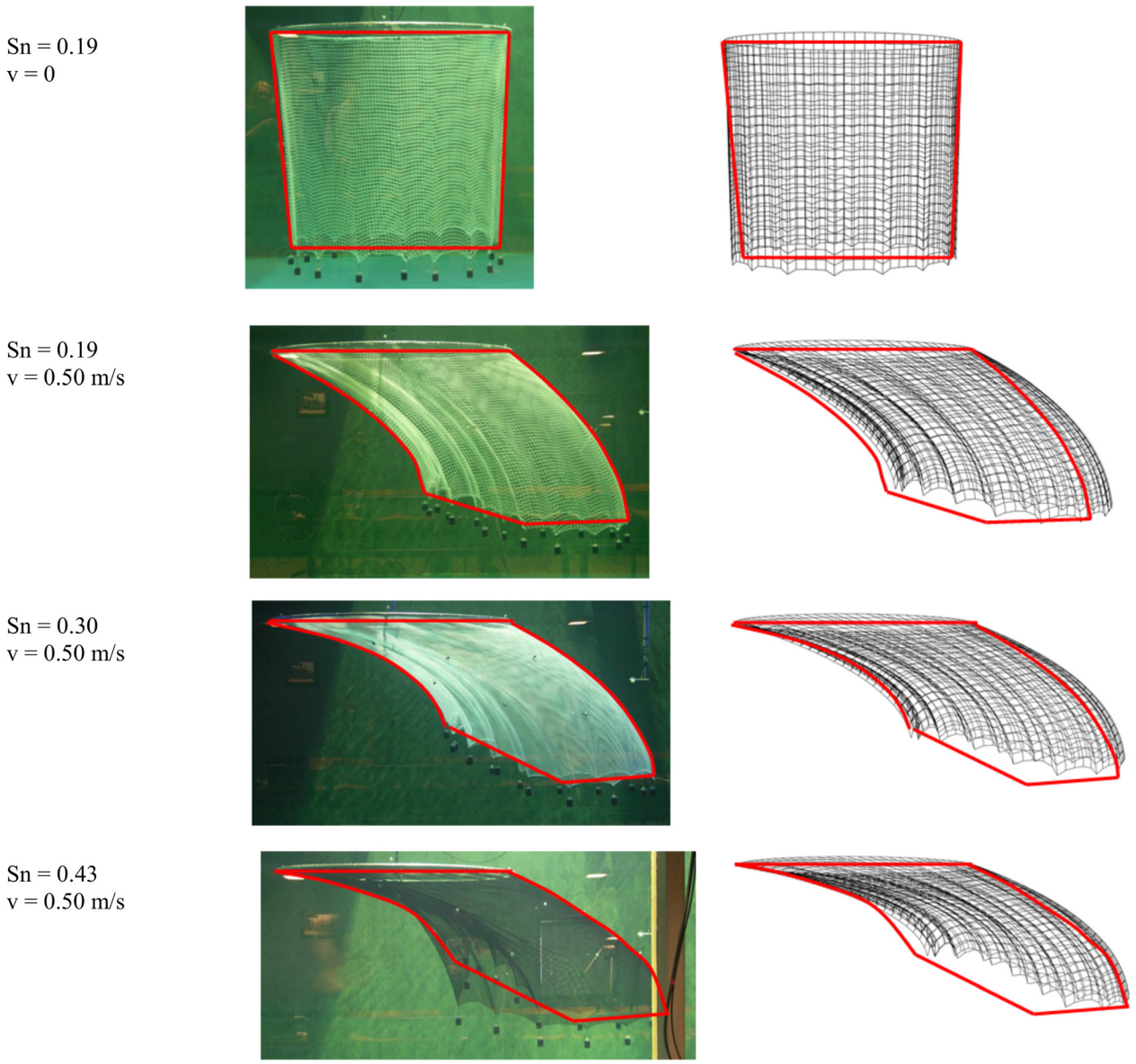

Fig. 8 Comparison of shape of physical model and modified truss method model subjected to $v = 0.5$ m/s

References

[1] Standards Norway, 2009, *NS 9415 Marine Fish Farms—Requirements for Site Survey, Risk Analyses, Design, Dimensioning, Production, Installation and Operation*.

[2] Moe, H., Fredheim, A., and Hopperstad, O. S., 2010, "Structural Analysis of Aquaculture Net Cages in Current," J. Fluids Struct., **26**(3), pp. 503–516.

[3] Moe, H., Olsen, A., Hopperstad, O. S., Jensen, Ø., and Fredheim, A., 2007, "Tensile Properties for Netting Materials Used in Aquaculture Net Cages," Aquacult. Eng., **37**(3), pp. 252–265.

[4] The International Organization for Standardization, 2002, *ISO 1107 Fishing Nets—Netting – Basic Terms and Definitions*.

[5] Gansel, L., 2011, "Average Flow Inside and Around Fish Cages With and Without Fouling in a Uniform Flow," ASME J. Offshore Mech. Arct. Eng., **134**(1), p. 011501.

[6] Kristiansen, T., and Faltinsen, O. M., 2012, "Modeling of Current Loads on Aquaculture Net Cages," J. Fluids Struct., **34**, pp. 218–235.

[7] Moe-Føre, H., Lader, P. F., Lien, E., and Hopperstad, O. S., 2015, "Measured and Calculated Loads on High Solidity Net Cages," (submitted).

[8] Løland, G., 1991, "Current Forces on Flow Through Fish Farms," Ph.D. thesis, The Norwegian Institute of Technology, Norway.

[9] Bloecher, N., Olsen, Y., and Guenther, J., 2013, "Variability of Biofouling Communities on Fish Cage Nets: A 1-Year Field Study at a Norwegian Salmon Farm," Aquaculture, **416–417**, pp. 302–309.

[10] Swift, M. R., Fredriksson, D. W., Unrein, A., Fullerton, B., Patursson, O., and Baldwin, K., 2006, "Drag Force Acting on Biofouled Net Panels," Aquacult. Eng., **35**(3), pp. 292–299.

[11] Zdravkovich, M. M., Brand, V. P., Mathew, G., and Weston, A., 1989, "Flow Past Short Circular Cylinders With Two Free Ends," J. Fluid Mech., **203**, pp. 557–575.

[12] Reite, K.-J., Aarsæther, K. G., Jensen, J., Kyllingstad, L. T., Johansen, V., Føre, M., Endresen, P. C., Kristiansen, D., Rundtop, P., and Fredheim, A., 2014, "FhSim-Time Domain Simulation of Marine Systems," ASME Paper No. OMAE2014-23165.

[13] Endresen, P. C., Føre, M., Fredheim, A., Kristiansen, D., and Enerhaug, B., 2013, "Numerical Modeling of Wake Effect on Aquaculture Nets," ASME Paper No. OMAE2013-11446.

[14] Moe, H., 2009, "Strength Analysis of Net Structures," Ph.D. thesis, 2009:48, Norwegian University of Science and Technology, Norway.

[15] Enerhaug, B., Føre, M., Endresen, P. C., Madsen, N., and Hansen, K., 2012, Current Loads on Net Panels With Rhombic Meshes, ASME Paper No. OMAE2012-83394.

[16] Priour, D., 1999, "Calculation of Net Shapes by the Finite Element Method With Triangular Elements," Commun. Numer. Methods Eng., **15**(10), pp. 757–765.

[17] Blevins, R. D., 2003, *Applied Fluid Dynamics Handbook*, Krieger Publishing Company, Malabar, FL.

[18] Fredheim, A., 2005, "Current Forces on Net Structures," Ph.D. thesis, Norwegian University of Science and Technology, Norway.

[19] Gjøsund, S. H., and Enerhaug, B., 2010, "Flow Through Nets and Trawls of Low Porosity," Ocean Eng., **37**(4), pp. 345–354.